Atmos. Chem. Phys. Discuss., doi:10.5194/acp-2016-515, 2016
Manuscript under review for journal Atmos. Chem. Phys.
Published: 19 July 2016

Atmospheric Chemistry and Physics Discussions

Air–surface exchange of gaseous mercury over permafrost soil: an investigation at a high-altitude (4700 m a.s.l.) and remote site in the central Qinghai-Tibet Plateau

Zhijia Ci[1], Fei Peng[2], Xian Xue[2], and Xiaoshan Zhang[1]

[1]Research Center for Eco-Environmental Sciences, Chinese Academy of Sciences, Beijing, 100085, China

[2]Cold and Arid Regions Environmental and Engineering Research Institute, Chinese Academy of Sciences, Lanzhou, 730000, China

Correspondence to: Z. J. Ci (zjci@rcees.ac.cn)

Abstract. The pattern of air–surface gaseous mercury (mainly Hg(0)) exchange in the Qinghai-Tibet Plateau (QTP) may be unique because this region is characterized by low temperature, great temperature variation, intensive solar radiation, and pronounced freeze-thaw process of permafrost soils. However, air–surface Hg(0) flux in the QTP is poorly investigated. In this study, we performed filed measurements and controlled field experiments with dynamic flux chambers technique to examine the flux, temporal variation and influencing factors of air–surface Hg(0) exchange at a high-altitude (4700 m a.s.l.) and remote site in the central QTP. The results of field measurements showed that surface soils were net emission source of Hg(0) in the entire study. Hg(0) flux showed remarkable seasonality with net high emission in the warm campaigns and net low deposition in winter campaign, and also showed the diurnal pattern with emission in daytime and deposition in nighttime, especially on days without precipitation. Rainfall events on the dry soils induced large and immediate increase in Hg(0) emission. Snowfall events did not induce the pulse of Hg(0) emission, but snow melt resulted in the immediate increase in Hg(0) emission. Daily Hg(0) fluxes on rainy or snowy days were higher than those of days without precipitation. Controlled field experiments suggested that water addition to dry soils significantly increased Hg(0) emission both in short and relatively long timescales, and also showed that UV radiation was primarily attributed to Hg(0) emission in the daytime. Our findings imply that a warm climate and environmental change could facilitate Hg release from the permafrost terrestrial ecosystem in the QTP.

Atmos. Chem. Phys. Discuss., doi:10.5194/acp-2016-515, 2016
Manuscript under review for journal Atmos. Chem. Phys.
Published: 19 July 2016

Atmospheric Chemistry and Physics Discussions

1 Introduction

Soils represent the largest Hg reservoirs in ecosystems and play a major role in the global Hg cycle (Selin, 2009; Agnan et al., 2016). Background soils receive Hg input from atmospheric deposition, which is mainly retained in organic-rich layers of upper soils (Schuster, 1991; Khwaja et al., 2006). Under favorable conditions, Hg in soils can be reduced to Hg(0) and then emitted to the overlaying air because of its high volatility (Schlüter, 2006). Therefore, soils can serve as both sources and sinks of atmospheric Hg (Pirrone and Mason, 2009; Amos et al., 2013; Agnan et al., 2016).

In the past several decades, efforts have been made to improve the understanding of soil Hg biogeochemistry (Zhang and Lindberg, 1999; Lin et al., 2010; Schlüter, 2006; Jiskra et al., 2015). Measurements across various types of soils and climates show that air–soil Hg(0) exchange has highly spatial and temporal variation and bidirectional exchange behavior (Agnan et al., 2016 and references therein). Field measurements and laboratory experiments highlight that various factors and processes influence air–surface Hg(0) exchange, including concentrations and species of soil Hg (Gustin et al., 1999, 2002; Hintelmann et al., 2002; Bahlmann et al., 2006; Kocman and Horvat, 2010; Eckley et al., 2011; Edwards and Howard, 2013; Mazur et al., 2015), solar radiation (Gustin et al., 2002; Moore and Carpi, 2005; Gustin et al., 2006; Xin et al., 2007; Fu et al., 2008a; Kocman and Horvat, 2010; Park et al., 2014), precipitation (Lindberg et al., 1999; Gustin and Stamenkovic, 2005; Gabriel et al., 2011), soil temperature and moisture (Gustin et al., 1997; Gustin and Stamenkovic, 2005; Ericksen et al., 2006; Xin et al., 2007; Briggs and Gustin, 2013; Park et al., 2014; Mazur et al., 2015), soil organic matter and pH (Yang et al., 2007; Xin and Gustin, 2007; Mauclair et al., 2008); land cover (Dommergue et al., 2003; Ericksen et al., 2005; Cobbett et al., 2007; Gabriel and Williamson, 2008; Zhu et al., 2011; Durnford et al., 2012a, b; Toyota et al., 2014a, b); atmospheric Hg(0) concentrations and other chemical compositions (Engle et al., 2004; Xin and Gustin, 2007; Fu et al., 2008a), biological activity (Choi and Holsen, 2009), as well as atmospheric turbulence (Gustin et al., 1997; Poissant et al. 1999). Existing studies on Hg(0) dynamics at air–surface interface are mainly performed in temperate regions (Agnan et al., 2016 and reference therein). The seasonal frozen soils and permafrost widely distribute, accounting for almost 70% of terrestrial area of Earth (NSIDC). However, the knowledge of air–surface Hg(0)

Atmos. Chem. Phys. Discuss., doi:10.5194/acp-2016-515, 2016
Manuscript under review for journal Atmos. Chem. Phys.
Published: 19 July 2016

Atmospheric Chemistry and Physics Discussions

dynamics in cold region is limited (Cobbett et al., 2007; Durnford and Dastoor, 2011). Most current parameters of air–soil Hg(0) exchange applied in Hg biogeochemical models are mainly derived from temperate regions of North America and Europe (Zhu et al., 2016).

The Qinghai-Tibet Plateau (QTP) is located in the western China with the area of 2.5 million km^2 and mean altitude of > 4000 m. Due to the high altitude and subsequent low temperature, a significant portion (~ 1.5 million km^{-2}) of the QTP is underlain by permafrost (Kang et al., 2010). Because of the harsh natural environment, limited research resources and difficulty of access and sampling logistics, studies on Hg biogeochemistry in the QTP are limited. The role of QTP in the regional and global Hg biogeochemical cycle is poorly understood (Ci et al., 2012; Agnan et al., 2016). At present, Hg studies in the QTP mainly focused on the investigations of Hg concentration, speciation and distribution in environmental samples, such as air (Fu et al., 2008b; 2012; Yin et al., 2015), snow and glacier (Loewen et al., 2007; Wang et al., 2008; Zhang et al., 2012; Huang et al., 2012), and rain water (Huang et al., 2013). The knowledge of Hg(0) dynamics at air–surface interface in the QTP is extremely poor. The unique climatic condition, land cover and soil property suggest the need for the specific air–soil Hg(0) flux data and mechanism representative of the environmental setting in the QTP to better constrain global natural sources inventories (Ci et al., 2012; Agnan et al., 2016).

In this study, we applied dynamic flux chambers (DFCs) technique to investigate the flux, temporal variation and influencing factors of air–surface Hg(0) exchange at a representative research station in the central QTP. Meanwhile, controlled field experiments were performed to explore the effect of rainfall and different wavebands of solar radiation on air–soil Hg(0) flux. Combining the result of this study and other knowledge, we discuss the effect of future climatic and environmental change on air–surface Hg(0) dynamics in the QTP.

2 Methods

2.1 Study site

The study was performed at the Beiluhe Permafrost Engineering and Environmental Research Station affiliated to the Cold and Arid Regions Environmental and Engineering Research Institute,

Atmos. Chem. Phys. Discuss., doi:10.5194/acp-2016-515, 2016
Manuscript under review for journal Atmos. Chem. Phys.
Published: 19 July 2016

Chinese Academy of Sciences (CAREER–CAS). The elevation of the Beiluhe region is about 4700 to 4800 m a.s.l.. The station (34° 49' 45" N, 92° 56' 06" E) lies over the continuous permafrost zone in the central QTP (Fig. 1). The terrain is undulation with sparse vegetation and surface fine sands or gravels. The thickness of the active layer and permafrost around the station is 2.0–3.2 m and 60–200 m, respectively; the active layer begins to freeze in September and thaw in May (Peng et al., 2015a). The Beiluhe region experiences a continental climate with cold winter (up to –30 ℃) and warm summer (up to 25 ℃). The magnitude of daily air temperature is up to 30 ℃, and the annual mean surface air temperature is about –2 to –3 ℃ (Peng et al., 2015a). The solar radiation is high and characterized by intense UV radiation (Wei et al., 2006). The mean annual precipitation is about 300 mm and mostly occurs during the May to October under the influence of the Southern Asian Monsoon; the annual potential evapotranspiration (~1300 mm) greatly exceeds the precipitation (Peng et al., 2015a). As a remote region, there is no direct human activity to influence the local Hg cycle.

2.2 Measurement of air–surface Hg(0) flux

The dynamic flux chambers (DFCs) technique was widely used to investigate Hg(0) flux between air–surface interface because it is inexpensive, portable, easy to set up and operate (e.g., Kim and Lindberg, 1995; Carpi and Lindberg, 1998; Gustin et al., 2006; Wang et al., 2006; Dommergue et al., 2007; Fu et al., 2008a; Kocman and Horvat, 2010; Edwards and Howard, 2013). The principle for measuring air–surface Hg(0) flux using the DFCs technique involves placing a chamber over a surface and measuring the difference in air Hg(0) concentrations at inside and outside of the chamber. DFC means continuously draw ambient air into the chamber through inlets at a set flushing flow rate. Air–surface Hg(0) flux was calculated using Eq. (1),

$$F = Q\frac{C_0 - C_i}{A} \quad \text{(Eq. 1)}$$

where F is the Hg(0) flux (ng m^{-2} h^{-1}), Q is the flushing flow through the chamber (m^3 h^{-1}), A is the footprint of the chamber (m^2), C_0 and C_i (ng m^{-3}) is air Hg(0) concentrations at outlet and inlet of the chamber, respectively. Positive flux values indicate Hg(0) emission from the surface into the air; negative flux values represent Hg(0) deposition to the surface from the air. The advantage and

Atmos. Chem. Phys. Discuss., doi:10.5194/acp-2016-515, 2016
Manuscript under review for journal Atmos. Chem. Phys.
Published: 19 July 2016

Atmospheric Chemistry and Physics Discussions

limitation of DFCs technique for determining Hg(0) flux have been extensively discussed in previous studies (e.g., Wallschläger et al., 1999; Gillis and Miller, 2000; Lindberg et al., 2002; Eckley et al., 2010; Lin et al., 2012; Sommar et al., 2012; Zhu et al., 2015a, b).

In this study, quartz chambers were constructed for measuring Hg(0) flux and exploring the effect of different rainfall depths and radiation condition on the Hg(0) flux. Quartz glass has many advantages as construction material of chamber for determining Hg(0) flux in background soils. First, it has high transmittance of the full spectrum of solar radiation, especially UV waveband (Fig. S1 in Supplement). Therefore, quartz chamber is suitable to determine the more "actual" Hg(0) flux because the short wavelength of solar radiation has been found to have important effect on Hg(0) dynamics at the air–soil interface (Moore and Carpi, 2005; Bahlmann et al., 2006). Second, it has low potential for Hg(0) adsorption and is easy to clean by heating to remove Hg bonding on the surface (Ci et al., 2016a). This will decrease the systematic blank of measurement, which is critical for investigating Hg(0) flux over background soils (Carpi and Lindberg, 1998).

Our semi-cylindrical quartz chamber was 8 cm high and 24 cm length with a footprint of 0.0384 m^{-2} (0.16 m x 0.24 m) and an internal volume of 2.41 L, which is similar to previous studies (Eckley et al., 2010 and reference therein). The chamber had nine inlets (8 mm in diameter) and three outlets which were on the two opposite section of the chamber. The inlet sampling tube was placed near the ground surface (3 cm above the surface) directly near the inlet of the chamber. A flushing ambient air was drawn by vacuum pump (KNF, Inc. Germany) with 3.0 L min^{-1} (0.18 m^3 h^{-1}) through the chamber.

Since the harsh environment condition and the unstable power supply, the usage of the commercial automatic Hg analyzer (such as Tekran 2537) to conduct filed measurements of Hg(0) flux is challenging in the Beiluhe station. Therefore, air Hg(0) concentrations in both inlet and outlet of the chamber were monitored manually by gold trap simultaneously with a 2–3 h intervals (Ci et al., 2016b). The air was pumped through gold trap using air pump (KNF, Inc. Germany) with 0.50 L min^{-1} (0.03 m^3 h^{-1}). Hg(0) collected on gold traps was quantified on site by a cold vapor atomic fluorescence spectrophotometer (CVAFS, Model III, Brooks Rand, USA) using two-stage gold amalgamation method (Fitzgerald and Gill, 1979; Ci et al., 2011, 2016a). Gold trap efficiencies were determined in

Atmos. Chem. Phys. Discuss., doi:10.5194/acp-2016-515, 2016
Manuscript under review for journal Atmos. Chem. Phys.
Published: 19 July 2016

Atmospheric Chemistry and Physics Discussions

laboratory (Hg(0) concentration: 3.2 to 13.4 ng m^{-3}) and field (Hg(0) concentration: ~1 to 2 ng m^{-3} to 9.4 ng m^{-3}), and multiple measurements using gold traps in series showed no breakthrough at the sample flow rate of 0.50 L min^{-1} for 5 hours. The method detection limit was 0.03 ng m^{-3} and precision was 3±2%.

The turnover time obtained from this protocol was 0.68 min, which is similar to previous studies (Eckley et al., 2010 and reference therein). The flow rates of air both the inlet and outlet of chamber were adjusted by a needle valve and controlled by a rotameter. Prior to the measurement, the rotameters were calibrated by a mass flow meter and a volumetric gas meter. The accuracy of flow rate was ±3%. The sampling control system was installed in the tent near the soil plot (<2 m).

In this study, a bare soil plot of 2 x 2 m was chosen and separated to four subplots (1 x 1 m, labeled as Subplot A to D) to measure Hg(0) flux and further to investigate the effects of different wavelengths of solar radiation on the Hg(0) exchange. Geologic unit of this soil plot is representative of major lithologic units of the Beiluhe region. The study was conducted in four campaigns (May, September, and December 2014 and May–June 2015), covering typical intra-annual meteorological condition in the study region. It is well-known that the application of the chamber isolates the soil surface from air turbulence and rain/dew/frost/snow, altering many environmental parameters that influence Hg(0) production/consumption and deposition/emission at air–soil interface (Sommar et al., 2012 and references therein). In the Beiluhe region, the rain/snow/dew/frost commonly occurs in short time scale (10^1–10^2 minutes) because of the high-altitude location and great variation of temperature and unstable weather conditions. To minimize the effect of great variation of soil surface condition on Hg(0) flux measurements, when only to measure Hg(0) flux, we used the same chamber to measure Hg(0) flux in four subplots (Subplot A to D) in turn. For the rainy and snowy days, if possible, the chamber was moved to next subplot generally after the rain or snow because studies confirmed the significant influence of precipitation on Hg(0) flux in short time scale (Lindberg et al., 1999; Gustin and Stamenkovic, 2005; Johnson et al., 2003; Song and Van Heyst, 2005; Lalonde et al., 2001, 2003; Dommergue et al., 2003, 2007, 2012; Fa ṅ et al., 2007; Bartels-Rausch et al., 2008; Brooks et al., 2008; Mann et al., 2014, 2015). For the days without precipitation, the chamber was moved to next subplot before sunrise to capture the effect of frost or dew on air–surface Hg(0) flux in the light.

Atmos. Chem. Phys. Discuss., doi:10.5194/acp-2016-515, 2016
Manuscript under review for journal Atmos. Chem. Phys.
Published: 19 July 2016

In this study, all materials in contact with Hg(0) were quartz, Teflon or borosilicate glass. The chambers and tubing were rigorously acid washed (Ci et al., 2016a). The quartz chambers were heated to 650 ℃ for 2 h prior the measurement to further remove all Hg (Ci et al., 2016a). System blanks of the four chamber systems were systemically inspected on site by placing acid-cleaned Teflon filter beneath the chamber and routinely inspected before and after the measurements under the field condition. The overall blank results were taken as the average of all chamber blanks for each particular day or from the entire period if continuous monitoring was conducted. The blank values of the four chambers were found to be very low (mean ± SD: –0.02 ± 0.03 ng m^{-2} h^{-1}; range: –0.20–0.07 ng m^{-2} h^{-1}) and were not significantly different ($p>0.05$) throughout the entire study. We also found that the mean blank values were not significantly different ($p>0.05$) from zero and were insignificant compared to the measured Hg(0) fluxes (see below), then Hg(0) flux data was not blank-corrected in this study.

2.3 Determination of soil Hg

Surface soil samples (0–2 cm) were collected from four soil subplots during June 2014 campaign. Soil samples were freeze-dried and homogenized for total Hg determination using a Milestone's DMA direct Hg analyzer (detection limit: 0.01 ng Hg or 0.15 ug kg^{-1}) following the EPA Method 7473 (Briggs and Gustin, 2013), and the analytical accuracy was 3%.

2.4 Measurements of environmental variables

A meteorological station that located 60 m from the soil plot was used to collect the following environmental variables: air temperature (℃), relative humidity (%), wind speed (m s^{-1}), precipitation (mm), photosynthetically active radiation (PAR, μ mol m^{-2} s^{-1}), surface soil temperature (℃). The surface soil temperature was monitored by an ASI-111 Precision Infrared Radiometer (Campbell Scientific Inc. USA). This sensor was installed on a bar 0.8 m above the soil surface and provided a non-contact measurement of the surface temperature. We also measured the soil temperature at 1.0 cm soil depth at the inside of chamber, and no significant difference was found between the soil temperature in the outside and inside of chamber. Details on the measurements of environmental variables are given in Peng et al. (2015a). The thickness of snowpack was measured manually.

3 Results and Discussion

Atmos. Chem. Phys. Discuss., doi:10.5194/acp-2016-515, 2016
Manuscript under review for journal Atmos. Chem. Phys.
Published: 19 July 2016

Atmospheric Chemistry and Physics Discussions

188 **3.1 Soil Hg**

189 Soil Hg concentrations of four subplots varied from 13.11 ± 0.51 to 12.83 ± 0.81 μg kg^{-1},
190 suggesting that the study region is a typical background soil for Hg. Soil Hg concentrations and air–soil
191 Hg(0) flux of four subplots were not statistically different ($p>0.05$), indicating the properties of the soil
192 plot were homogeneous.

193 **3.2 Hg(0) in ambient air**

194 Figure 2 shows the temporal variation of air Hg(0) concentrations inside and outside of chamber,
195 air–surface Hg(0) flux and environmental variables during four campaigns in 2014–2015. Hg(0)
196 concentrations of ambient air ranged from 0.93 to 1.78 ng m^{-3} with a mean of 1.36 ± 0.17 ng m^{-3}
197 (n=361), which were slightly lower than those in typical Northern Hemisphere background region (~1.5
198 ng m^{-3}, Sprovieri et al., 2007; Ebinghaus et al., 2011). To our knowledge, four measurements (including
199 this study) have been conducted to determine atmospheric Hg over the QTP (see Fig. 1 for the
200 locations). The gradient of atmospheric Hg(0) over the QTP was characterized by high concentrations in
201 Mt. Gongga (3.98 ± 1.62 ng m^{-3}, Fu et al., 2008b) and Mt. Waliguan (1.98 ± 0.98 ng m^{-3}, Fu et al.,
202 2012), moderate concentrations in the Beiluhe (1.36 ± 0.17 ng m^{-3}, this study), and low concentrations
203 in the Nam Co (0.96 ± 0.19 ng m^{-3}, Yin et al., 2015). It seems that the sampling station with relatively
204 long distance from the source region of atmospheric Hg(0) (i.e., the Central China, Streets et al., 2005)
205 had relatively low atmospheric Hg(0) concentrations (Fig. 1). Atmospheric Hg(0) concentrations were
206 high in three warm campaigns and low in winter campaign in the Beiluhe station (Fig. 3), which is
207 consistent with Mt. Gongga (Fu et al., 2008b) and Mt. Waliguan (Fu et al., 2012).

208 **3.3 Air–surface Hg(0) flux and influencing factors**

209 **3.3.1 Temporal variation of Hg(0) flux**

210 The mean of air–surface Hg(0) flux in the entire study period were 2.86 ng m^{-2} h^{-1} (25.05 μg m^{-2} y^{-1}
211), indicating that surface soils were net emission source of Hg(0). Hg(0) flux in this study is
212 comparable to those over background soils (–10–10 ng m^{-2} h^{-1}, Wang et al., 2006; Ericksen et al., 2006;
213 Fu et al., 2008a), but greatly lower than those over Hg-enriched soils (10^2–10^3 ng m^{-2} h^{-1}, Gustin et al.,

Atmos. Chem. Phys. Discuss., doi:10.5194/acp-2016-515, 2016
Manuscript under review for journal Atmos. Chem. Phys.
Published: 19 July 2016

1999; Wang et al., 2007; Edwards and Howard, 2013), indicating that soil Hg concentrations may be the dominant factor for controlling the magnitude of Hg(0) emission flux (Agnan et al., 2016 and reference therein).

Figure 2 shows that the Hg(0) flux was highly variable. The highest Hg(0) emission fluxes of 28.46 ng m^{-2} h^{-1} were observed at 13:00–15:00 on 13 September 2014 after a rain event on dry soils. The highest Hg(0) deposition fluxes of –6.24 ng m^{-2} h^{-1} were observed at nighttime over the cold and dry surface soil during December 2014 campaign (03:30–06:30, 24 December 2014).

Hg(0) flux generally showed the diurnal pattern with high emission in daytime and remarkable deposition in nighttime, especially on days without precipitation (Fig. 2). Many studies have confirmed that solar radiation is one of the most important drivers for soil Hg(0) emission (Xin and Gustin, 2007; Choi and Holsen, 2009; Kocman and Horvat, 2010); high surface temperature also facilitates Hg(0) production and subsequent emission (Park et al., 2014). Therefore, the two environmental variables jointly regulate the diurnal pattern of Hg(0) flux. An in-depth discussion on synergistic effects of solar radiation and surface temperature on Hg(0) flux is provided in below. Interestingly, the diurnal pattern of Hg(0) flux of each day during December 2014 campaign was almost identical, which may be associated with very similar weather conditions throughout the entire campaign.

Hg(0) flux showed pronounced seasonality with high emission in three warm campaigns and net low deposition during winter campaign (Fig. 3). Similar seasonality has been reported in many other studies (e.g., Gabriel et al., 2006). As discussed below, in warm seasons, some environmental variables, such as high solar radiation, surface temperature and precipitation, facilitate the soil Hg(0) emission.

3.3.2 Effect of precipitation (rain and snow) on air–surface Hg(0) flux

Many studies addressed that precipitation greatly influences air–surface Hg(0) flux over different timescales (Lindberg et al., 1999). In previous studies, investigators mainly focused on the effect of rainfall/watering on air–soil Hg(0) flux (Lindberg et al., 1999; Johnson et al., 2003; Gustin and Stamenkovic, 2005; Song and Van Heyst, 2005; Corbett-Hains et al., 2012) or the fate and transport of Hg(0) at air–snow interface (Lalonde et al., 2001, 2003; Ferrari et al., 2005; Dommergue et al., 2003, 2007; Fa ̈n et al., 2007; Bartels-Rausch et al., 2008; Brooks et al., 2008; Steen et al., 2009; Durnford et

Atmos. Chem. Phys. Discuss., doi:10.5194/acp-2016-515, 2016
Manuscript under review for journal Atmos. Chem. Phys.
Published: 19 July 2016

Atmospheric Chemistry and Physics Discussions

al., 2012a, b; Mann et al., 2015). The field study on the effect of snowmelt on Hg(0) flux is very limited (Cobbett et al., 2007). The precipitation at the Beiluhe station mainly occurs during May to October (Peng et al., 2015a). Due to the high-altitude location of the Beiluhe station, snow event commonly occurs in May to June and late September to October. Because of intensive solar radiation and surface temperature, the snow melts or sublimates in short time scale (10^0–10^2 hour), i.e., little/no snow accumulation occurs for long time (>3 day). Therefore, the Beiluhe region provides an unique opportunity to investigate the different effects of rain, snow, and snowmelt on the air–surface Hg(0) flux over different timescales.

Firstly, the effect of rain events on Hg(0) flux was investigated. Many studies reported that the rainfall or watering of dry soils can promote soil Hg(0) emission immediately (Lindberg et al., 1999; Gustin and Stamenkovic, 2005). We also found that the Hg(0) emission flux increased immediately following the rainfall (Fig. 2). This finding is consistent with many other studies (Gustin and Stamenkovic, 2005; Johnson et al., 2003; Lindberg et al., 1999; Song and Van Heyst, 2005). Investigators supposed that the dramatic increases in Hg(0) emission may be attributed to the physical displacement of Hg(0) present in soil air and desorption of loosely bound Hg(0) on soil particles by the infiltrating water (Johnson et al., 2003; Gustin and Stamenkovic, 2005). Notably, Fig. 2 displays that the pulse of Hg(0) emission after the rainfall was also observed at nighttime (such as 0:00 to 01:00 on 4 September 2014). Similar phenomenon was also documented by our controlled experiments (see below). This indicates that the immediate increase in Hg(0) emission might not be controlled by photochemical processes but by physical processes.

Soil moisture condition may also significantly regulate Hg(0) flux over relatively long timescales (from hours to several days). Therefore, many experiments studied the effect of water addition on the magnitude and pattern of air–soil Hg(0) flux over different timescales (Johnson et al., 2003; Gustin and Stamenkovic, 2005). However, most of studies were performed in controlled laboratory or mesocosm settings under certain well-defined, but not necessarily environment relevant conditions (Johnson et al., 2003; Gustin et al., 2004; Gustin and Stamenkovic, 2005; Song and Van Heyst, 2005; Kocman and Horvat, 2010; Corbett-Hains et al., 2012; Park et al., 2014). In this study, it was also challenging to reveal the effect of rainfall on Hg(0) flux over relatively long timescales via field measurement since

Atmos. Chem. Phys. Discuss., doi:10.5194/acp-2016-515, 2016
Manuscript under review for journal Atmos. Chem. Phys.
Published: 19 July 2016

the intermittent rain events occurred irregularly during June 2014 and September 2014 campaign (Fig. 2). For a better understanding of the effect of water addition, we chosen another similar soil plot with homogeneous soil property to conduct controlled field experiments to explore the effect of different rainfall depths on Hg(0) flux over different timescales (from minutes to hours). The controlled experiments were performed during May–June 2015 campaign since this period had high surface temperature and low precipitation (Fig. 2). In the Beiluhe station, hourly rainfall depth rarely exceeds 15 mm (Peng et al., 2015a). Therefore, we designed four different treatments of rainfall depth (0 mm, 1 mm, 5 mm, and 15 mm). The water addition to the dry soils commenced at night (01:40) on 30 May 2015 to exclude the effect of photochemical process in the first hours of experiments. We added the Milli-Q water (Hg concentration < 0.2 ng L^{-1}) to the inside and outside of the chamber by pre-clean plastic syringe within 10 min to simulate the three different rain depths. Four chambers were used to simultaneously measure Hg(0) flux over these four treatments for 22 hours (from 01:00 to 23:00) with the same protocol described in the Methods section. Hg(0) flux was measured with 20 min intervals in the first hours (from 01:00 to 04:20) of the experiments to investigate the temporal variation of Hg(0) flux in the short timescale, and with 1 hour intervals for the rest period of the experiments.

The high-time resolution measurements captured the immediate and dramatic increases in Hg(0) emission flux after the watering of dry soils (Fig. 4). The baseline Hg(0) flux of 0 mm treatment was used as the benchmark for the different rainfall depth treatments to be compared against. Obviously, the higher amount of water addition resulted in longer duration and higher accumulative flux of Hg(0) emission pulse. The duration of Hg(0) emission pulse for 1 mm and 5 mm treatment was < 20 min (from 01:40 to 02:00) and ~40 min (from 01:40 to 02:20), respectively, which was lower than that of 15 mm treatment (~80 min, from 01:40 to 03:00). The duration of Hg(0) emission for 15 mm treatment in the daytime was also longer than that of 1 mm and 5 mm treatment (Fig. 4).

As shown in Fig. 4, the cumulative flux of Hg(0) emission during the entire study period mainly included two fractions: the pulse of Hg(0) emission after the watering (i.e., emission flux by watering), and the Hg(0) emission during the daytime (i.e., emission flux by radiation). Figure 5 displays that both "emission flux by watering" and "emission flux by radiation" for 15 mm treatment were significantly higher than those of 1 mm and 5 mm treatment. As mentioned above, the dramatic increase in Hg(0)

Atmos. Chem. Phys. Discuss., doi:10.5194/acp-2016-515, 2016
Manuscript under review for journal Atmos. Chem. Phys.
Published: 19 July 2016

297 emission after the simulated rain can be explained by physical displacement of interstitial soil air by the
298 infiltrating water. The long emission duration and large immediate emission flux for soil plot with high
299 water addition can be explained by that the more water needed longer time to percolate the soil column
300 and displaced more soil Hg(0). Many previous studies suggested that the magnitude of Hg(0) emission
301 with a rainfall or stimulated rain depended on soil moisture condition, i.e., if the amounts of water
302 received by the soils was less than needed to saturate, the soil surface showed an immediate increase in
303 Hg(0) emission; after the soil became saturated, Hg(0) emission from surface soil was suppressed
304 (Klusman and Webster, 1981; Lindberg et al., 1999; Johnson et al., 2003; Gustin and Stamenkovic,
305 2005). In this study, the pulse of Hg(0) emission flux for 15 mm treatment was significantly higher than
306 that of 5 mm and 1 mm treatment (Fig. 5). The field water capacity and bulk density of soil in the
307 Beiluhe region is about 28% and 1 g cm^{-3} (Peng et al., 2015b), indicating that the 5 mm treatment may
308 induce the upper soil to saturate in short timescale since the duration of water addition was short (< 10
309 min). However, the pulse of Hg(0) emission for 15 mm treatment was significantly higher than that of 5
310 mm treatment. The surface soils with high sand content in the Beiluhe region have a high rate of water
311 infiltration and subsequently great infiltration depth. This process potentially increases the displacement
312 of soil Hg(0) and facilitates Hg(0) emission, as mentioned above. Therefore, in the field condition, the
313 duration and flux of pulse Hg(0) emission following water addition depends not only on how much
314 water received and soil moisture condition but also soil texture and soil water dynamics.

315 The water addition also increased the Hg(0) emission in the daytime, showing more water added,
316 longer duration of Hg(0) emission, and more Hg(0) emitted (Fig. 4 and Fig. 5). After the surface soil
317 was visibly dry, Hg(0) flux over soil plots with water addition had no significant difference from that of
318 the soil plot without water addition (i.e., 0 mm treatment). This result is consistent with many other
319 controlled studies. For example, Gustin and colleagues (Johnson et al., 2003; Gustin and Stamenkovic,
320 2005) found that once the soil water content became less than saturated, Hg(0) emission flux would be
321 significantly enhanced especially during the daytime, and once sufficient drying occured, the magnitude
322 of Hg(0) emission flux tended to gradually decrease. Investigators suggested that as the water
323 evaporates and soil dries, capillary action drives the upward movement of water and chemicals
324 (including Hg components) and recharge the Hg pool in surface soils (i.e., the “wick effect”) and

Atmos. Chem. Phys. Discuss., doi:10.5194/acp-2016-515, 2016
Manuscript under review for journal Atmos. Chem. Phys.
Published: 19 July 2016

subsequently favors the Hg(0) production and emission via photochemical processes in the light (Gustin and Stamenkovic, 2005). In our study, even for the wettest soil plot (i.e., 15 mm treatment), the surface soils were visually unsaturated in the daytime because of the low water retention, high infiltration rate of local soils and intensive solar radiation. Therefore, the pattern of Hg(0) emission for soil plots with high water addition is comparable to those of the above-mentioned studies.

Secondly, the effect of snow events on Hg(0) flux were investigated. One of the most significant differences between the rainfall and snowfall on the effect of Hg(0) exchange was that the snowfall did not induce the remarkable pulse of Hg(0) emission. For example, at 10:10 on 11 June 2014, a heavy snowfall occurred and continued to 11:20. The great thickness of snowpack reached to ~12 cm. However, no remarkable pulse of Hg(0) emission was observed during the snowfall. Instead, the Hg(0) dynamics at air–snow interface showed the clear diurnal pattern with high emission in daytime and deposition or emission albeit rather small in nighttime. This finding is consistent with previous studies on air–snow interface (Cobbett et al., 2007). It can be seen that the pattern of Hg(0) dynamics at air–snow interface was similar with that at air–soil interface, indicating that Hg(0) emission from surface snow was also mainly regulated by photochemical processes (Ferrari et al., 2005; Dommergue et al., 2003, 2007). However, it is well-known that the snowpack is a porous matrix, and gases are subjected to diffusion in the snowpack. Therefore, our measurements of Hg(0) flux at air–snow interface did not exclude the effect of Hg(0) dynamics at soil–snow interface, especially the low thickness (< 12 cm) of snowpack in the study.

We found that the snow melting led to the remarkable peak of Hg(0) emission. For example, during the sunrise of 12 June 2014, a precipitation with rain and snow induced the snowpack (12 cm) to melt suddenly and completely (i.e., the bare soil with no surface snow), a pulse of Hg(0) emission (~8 ng m^{-2} h^{-1}) was observed, which was the largest Hg(0) emission flux during June 2014 campaign. We supposed that the great increase in Hg(0) emission by snowmelt in this study was consistent with the effect of rainfall, i.e., the displacement of soil Hg(0) during the snowmelt permeation of the soil column resulted in the dramatic increase in Hg(0) emission. At present, the study on the effect of snowpack melting on Hg(0) emission is limited. Cobbett et al. (2007) also found the remarkable increase in Hg(0) emission in Canadian Arctic during the snow melt, although the Hg(0) flux was relatively small.

Atmos. Chem. Phys. Discuss., doi:10.5194/acp-2016-515, 2016
Manuscript under review for journal Atmos. Chem. Phys.
Published: 19 July 2016

353 Finally, the effect of precipitation (including rain and snow) on daily Hg(0) flux was investigated.
354 The above-mentioned results and discussion suggest that the precipitation has great potential to
355 facilitate soil Hg(0) emission over different timescales via physical, chemical and biological processes.
356 The main processes include the displacement of soil Hg(0) by water, the "wick effect" to increase the
357 photo-reducible Hg(II) pool in surface soils, and the increased soil moisture to promote the biotic and
358 abiotic reduction of Hg(II). Another well-documented process is that the atmospheric wet deposition of
359 Hg will increase the Hg pool in surface soils and the newly deposited Hg is very active to reduce to
360 Hg(0) (Hintelmann et al., 2002), although our study did not focus on this issue. During June 2014
361 campaign, no precipitation occurred in the first two days (6–7 June 2014), but the rest days were
362 rainy/snowy days (Fig. 2). We tried to use the daily Hg(0) flux of the two sunny days as the benchmark
363 to compare with those of rainy/snowy days to investigate the effect of precipitation on the Hg(0) flux
364 over the timescale of one day. Figure 6 showed that the daily Hg(0) flux for rainy/snowy days were
365 higher (ranging from 16% to 154%) than the mean of the two sunny days. The result indicates that the
366 precipitation increased soil Hg(0) emission on the timescale of one day, although the low solar radiation
367 and temperature on rainy/snowy days would potentially decrease soil Hg(0) emission, as mentioned
368 above.

369 **3.3.3 Effect of solar radiation and soil temperature on air–surface Hg(0) flux**

370 Almost all laboratory experiments and field measurements, including this study, show that the high
371 solar radiation and elevated soil temperature synergistically facilitate the soil Hg(0) emission (Edwards
372 and Howard, 2013; Park et al., 2014). The following hypotheses have been proposed to explain the role
373 of solar radiation and temperature in promoting soil Hg(0) emission, including (1) solar radiation
374 promotes the photo-reduction of Hg(II) in surface soils to form Hg(0) in short time scale; (2) solar
375 radiation and high soil temperature reduce the apparent activation energy of Hg(0) desorption and
376 increase Hg(0) emission from surface soils; and (3) the high soil temperature favors the Hg(0)
377 production in soil column by biotic and abiotic processes (Carpi and Lindberg, 1998; Gustin et al.,
378 2002).

Atmos. Chem. Phys. Discuss., doi:10.5194/acp-2016-515, 2016
Manuscript under review for journal Atmos. Chem. Phys.
Published: 19 July 2016

Atmospheric Chemistry and Physics Discussions

Many studies used the Arrhenius equation (Eq. 2) to quantitatively investigate the relationship between soil temperature and Hg(0) flux.

$$F = \mathrm{A}e^{-Ea/RT} \text{ or } \ln(F) = \ln(A) - \frac{Ea}{RT} \quad \text{(Eq. 2)}$$

where F is the Hg(0) flux (ng m^{-2} h^{-1}), R is the gas constant, T is the soil temperature (K), A is the pre-exponential factor and Ea is the apparent activation energy. A plot of ln(F) versus 1/T obtains a straight line with intercept equal to the log of the A, and the slop equal to $-Ea/R$. Theoretically, the concept of the apparent Ea refers to the thermally controlled reaction. Therefore, Hg(0) flux induced by light and precipitation should be excluded from the correlation analysis. However, in many previous studies, especially for the field measurements, the bulk Hg(0) flux in the light was generally used to explore the contribution of solar radiation or temperature to Hg(0) flux and did not isolate the respective effect of the two factors (Fu et al., 2008a). This will systematically overestimate or underestimate the contribution of solar radiation and temperature on soil Hg(0) emission depending on the source or sink of soil for Hg(0) in the dark. Only in some controlled experiments, the separated data was used to explore the respective role of radiation and temperature in soil Hg(0) emission (e.g., Kocman and Horvat, 2010).

In this study, for respectively determining the contribution of solar radiation and temperature on the Hg(0) flux, besides Hg(0) flux was measured in the natural light, Hg(0) flux in the dark was also measured simultaneously with a foil-covered chamber. The temperature-corrected Hg(0) flux (i.e., bulk Hg(0) flux in the light – Hg(0) flux in the dark) in daytime (PAR > 0) was considered to be the contribution of the solar radiation. As mentioned above, the effect of precipitation should be excluded from the data set, therefore we only collected Hg(0) flux data on days without precipitation during December 2014 and May–June 2015 campaign.

Figure 7 displays the temporal variation of bulk Hg(0) flux in the light, Hg(0) flux in the dark, net Hg(0) flux in the light (i.e., bulk Hg(0) flux in the light – Hg(0) flux in the dark) and the environmental variables. Obviously, changes in solar radiation had a greater influence on soil Hg(0) flux than did changes in soil temperature. The data showed that the soil served as a Hg(0) sink during all study days

Atmos. Chem. Phys. Discuss., doi:10.5194/acp-2016-515, 2016
Manuscript under review for journal Atmos. Chem. Phys.
Published: 19 July 2016

405 in December 2014 campaign in the dark with high deposition flux in low soil temperature and low
406 deposition flux in high soil temperature. During study days of May–June 2015 campaign, the soils
407 served as a very low Hg(0) source in the midday with relatively high soil temperature. This finding is
408 consistent with many studies in background soils (Ericksen et al., 2006; Gustin et al., 2006; Fu et al.,
409 2008a; Edwards and Howard, 2013). It indicates that the soil temperature plays an important role in
410 Hg(0) dynamics at the air–soil interface, i.e., low soil temperature favors to absorb Hg(0) or reduce
411 Hg(0) emission.

412 After the temperature corrected, except for the midday of study days during May–June campaign,
413 the net Hg(0) flux in the light was higher than the bulk Hg(0) flux. The positive linear correlation was
414 found between cumulative PAR and cumulative Hg(0) flux in the daytime, although cumulative PAR
415 only explained ~28% of variation in cumulative Hg(0) flux in the daytime (Fig. S2 in Supplement).

416 We used the Hg(0) emission data set in the dark to calculate the *Ea* using the Arrhenius equation.
417 Since the soils in the dark was the sink of atmospheric Hg(0) in most of the study period, only limited
418 data set (n=9) can be used (Fig. S3 in Supplement). The *Ea/R* for Hg(0) emission from our remote soils
419 with extremely low Hg concentrations (~12 ug kg^{-1}) was 30.40. Table S1 in Supplement lists the *Ea/R*
420 for different soils with large variation of soil Hg concentrations, including this study, and shows that the
421 *Ea/R* of Hg(0) emission from soils with low Hg concentrations was higher than those of soils with high
422 Hg concentrations and significantly lower than that of theoretical value (7.31) of elemental Hg. It
423 indicates that surface soils with high Hg concentrations has great potential to emit Hg(0). This trend is
424 consistent with the laboratory study of Bahlmann et al. (2006), although the availability of Hg in soils
425 also significantly regulate Hg(0) emission (Bahlmann et al., 2006; Kocman and Horvat, 2010).

426 The QTP is characterized by high solar radiation with intense UV radiation. We further performed
427 the controlled experiment to quantify the role of different wavebands of solar radiation (UVB, UVA and
428 visible light) in Hg(0) flux. Figure 8 shows that UV radiation was the dominant waveband of solar
429 radiation for Hg(0) emission in the daytime, contributing >80% of Hg(0) emission in the light, and the
430 contribution of UV-B radiation accounted for >50% in all study days. This finding is consistent with
431 previous laboratory studies (Moore and Carpi, 2005; Bahlmann et al., 2006; Xin et al., 2007).

Atmos. Chem. Phys. Discuss., doi:10.5194/acp-2016-515, 2016
Manuscript under review for journal Atmos. Chem. Phys.
Published: 19 July 2016

Atmospheric Chemistry and Physics Discussions

4 Conclusions and implication

In this study, we measured the Hg(0) flux between the air and surface permafrost soil in the QTP. We also performed the controlled field experiments to explore the effect of precipitation and different wavebands of solar radiation on the Hg(0) exchange air–soil interface. The result showed that the environmental conditions, including solar radiation, soil temperature and precipitation, greatly influenced the Hg(0) exchange between air and surface.

This study and other field measurements and laboratory experiments have clarified that the fate and transport of soil Hg is very sensitive to the environmental variables (Krabbenhoft and Sunderland, 2013). Therefore, our results have several important implications to the Hg biogeochemical cycle in the soils of QTP under the rapid climate warming and environmental change. Firstly, the increased surface temperature in the QTP will potentially promote the remobilization of soil Hg. Field measurements and modeling study have revealed that the surface temperature in the QTP is increasing, and the warming trend exceeds those for the Northern Hemisphere and the same latitudinal zone (Kang et al., 2010). Secondly, the increased UV radiation in the QTP may improve Hg(0) emission from surface soils. UV radiation reaching the surface of the QTP is estimated to increase because of the decrease of stratospheric O_3 (Zhou et al., 2013). Our result and many above-mentioned studies show that UV radiation plays the primary role in promoting the surface Hg(0) emission in the daytime. Thirdly, the temp-spatial pattern of precipitation in the QTP is also altering (Kang et al., 2010), which potentially alters the flux and temp-spatial pattern of air–soil Hg(0) exchange in this region because of the importance of precipitation on the Hg(0) exchange. However, this study was just the beginning to explore the effect of climate change on the terrestrial Hg cycle in the QTP. The large uncertainties highlight that more researches are needed in the future.

Acknowledgements

The study was financially supported by the National Key Basic Research Program of China (No. 2013CB430002), National Natural Science Foundation of China (Nos. 41573117, 41371461, 41203068), and Young Scientists Fund of Research Center for Eco-Environmental Sciences, Chinese Academy of Sciences (No. RCEES-QN-20130048F). We thank the staff of the Beiluhe Permafrost Engineering and

Environmental Research Station affiliated to the Cold and Arid Regions Environmental and Engineering Research Institute, Chinese Academy of Sciences (CAREER–CAS) for their assistance.

References

Agnan, Y., Le Dantec, T., Moore, C. W., Edwards, G. C., and Obrist, D. New constraints on terrestrial surface–atmosphere fluxes of gaseous elemental mercury using a global database, Environ. Sci. Technol., 50, 507–524, 2016.

Amos, H. M., Jacob, D. J., Streets, D. G., and Sunderland, E. M. Legacy impacts of all-time anthropogenic emissions on the global mercury cycle, Global Biogeochem. Cy., 27, 410–421, 2013.

Bahlmann, E., Ebinghaus, R., and Ruck, W. Development and application of a laboratory flux measurement system (LFMS) for the investigation of the kinetics of mercury emissions from soils, J. Environ. Manage., 81, 114–125, 2006.

Bartels-Rausch, T., Huthwelker, T., Jöri, M., Gäggeler, H. W., and Ammann, M. Interaction of gaseous elemental mercury with snow surfaces: laboratory investigation, Environ. Res. Lett., 3, 52–55, 2008.

Briggs, C., and Gustin, M. S. Building upon the conceptual model for soil mercury flux: evidence of a link between moisture evaporation and Hg evasion, Water Air Soil Pollut., 224, 1–13, 2013.

Brooks, S., Arimoto, R., Lindberg, S., and Southworth, G. Antarctic polar plateau snow surface conversion of deposited oxidized mercury to gaseous elemental mercury with fractional long-term burial, Atmos. Environ., 42, 2877–2884, 2008.

Carpi, A., and Lindberg, S. E. Application of a Teflon™ dynamic flux chamber for quantifying soil mercury flux: tests and results over background soil, Atmos. Environ., 32, 873–882, 1998.

Choi, H. D., and Holsen, T. M. Gaseous mercury emissions from unsterilized and sterilized soils: the effect of temperature and UV radiation, Environ. Pollut., 157, 1673–1678, 2009.

Ci, Z. J., Zhang, X. S., Wang, Z. W., and Niu, Z. C. Phase speciation of mercury (Hg) in coastal water of the Yellow Sea, China, Mar. Chem., 126, 250–255, 2011.

Ci, Z. J., Zhang, X. S., Yin, Y. G., Chen, J. S., and Wang, S. W. Mercury redox chemistry in waters of the eastern Asian seas: from polluted coast to clean open ocean, Environ. Sci. Technol., 50, 2371–2380, 2016a.

Ci, Z. J., Zhang, X. S., and Wang, Z. W. Air–sea exchange of gaseous mercury in the tropical coast (Luhuitou fringing reef) of the South China Sea, the Hainan Island, China, Environ. Sci. Pollut. Res., 23, 11323–11329, 2016b.

Ci, Z. J., Zhang, X. S., and Wang, Z. W. Enhancing atmospheric mercury research in China to improve the current understanding of the global mercury cycle: the need for urgent and closely coordinated efforts, Environ. Sci. Technol., 46, 5636–5642, 2012.

493 Cobbett, F. D., Steffen, A., Lawson, G., and Van Heyst, B. J. GEM fluxes and atmospheric mercury
494 concentrations (GEM, RGM and Hgp) in the Canadian Arctic at Alert, Nunavut, Canada
495 (February–June 2005), Atmos. Environ., 41, 6527–6543, 2007.

496 Corbett-Hains, H., Walters, N. E., and Van Heyst, B. J. Evaluating the effects of sub-zero temperature
497 cycling on mercury flux from soils, Atmos. Environ., 63, 102–108, 2012.

498 Dommergue, A., Bahlmann, E., Ebinghaus, R., Ferrari, C., and Boutron, C. Laboratory simulation of
499 Hg^0 emissions from a snowpack, Anal. Bioanal. Chem., 388, 319–327, 2007.

500 Dommergue, A., Barret, M., Courteaud, J., Cristofanelli, P., Ferrari, C. P., and Gallée, H. Dynamic
501 recycling of gaseous elemental mercury in the boundary layer of the Antarctic Plateau, Atmos.
502 Chem. Phys., 12, 11027–11036, 2012.

503 Dommergue, A., Ferrari, C. P., Poissant, L., Gauchard, P. A., and Boutron, C. F. Diurnal cycles of
504 gaseous mercury within the snowpack at Kuujjuarapik/Whapmagoostui, Quebec, Canada, Environ.
505 Sci. Technol., 37, 3289–3297, 2003.

506 Durnford, D., and Dastoor, A. The behavior of mercury in the cryosphere: A review of what we know
507 from observations, J. Geophys. Res., 116, D06305, 2011.

508 Durnford, D. A., Dastoor, A. P., Steen, A. O., Berg, T., Ryzhkov, A., Figueras-Nieto, D., Hole, L. R.,
509 Pfaffhuber, K. A., and Hung, H.: How relevant is the deposition of mercury onto snowpacks? –
510 Part 1: A statistical study on the impact of environmental factors, Atmos. Chem. Phys., 12, 9221–
511 9249, 2012a.

512 Durnford, D., Dastoor, A., Ryzhkov, A., Poissant, L., Pilote, M., and Figueras-Nieto, D.: How relevant
513 is the deposition of mercury onto snowpacks? – Part 2: A modeling study, Atmos. Chem. Phys., 12,
514 9251–9274, 2012b.

515 Ebinghaus, R., Jennings, S. G., Kock, H. H., Derwent, R. G., Manning, A. J., and Spain, T. G.
516 Decreasing trends in total gaseous mercury observations in baseline air at Mace Head, Ireland from
517 1996 to 2009, Atmos. Environ., 45, 3475–3480, 2011.

518 Eckley, C. S., Gustin, M., Lin, C-J., Li, X., and Miller, M. B. The influence of dynamic chamber design
519 and operating parameters on calculated surface–to–air mercury fluxes, Atmos. Environ., 44, 194–
520 203, 2010.

521 Eckley, C. S., Gustin, M., Marsik, F., and Miller, M. B. Measurement of surface mercury fluxes at
522 active industrial gold mines in Nevada (USA), Sci. Total Environ., 409, 514–522, 2011.

523 Edwards, G. C., and Howard, D. A. Air–surface exchange measurements of gaseous elemental mercury
524 over naturally enriched and background terrestrial landscapes in Australia, Atmos. Chem. Phys., 13,
525 5325–5336, 2013.

526 Engle, M. A., Gustin, M. S., Lindberg, S. E., and Gerler, A. W. Investigation of the effect of
527 tropospheric oxidants on Hg emissions from substrates, Mater. Geoenviron., 51, 1546–1549, 2004.

528 Ericksen, J. A., Gustin, M. S., Lindberg, S. E., Olund, S. D., and Krabbenhoft, D. P. Assessing the
529 potential for re-emission of mercury deposited in precipitation from arid soils using a stable
530 isotope, Environ. Sci. Technol., 39, 8001–8007, 2005.

531 Ericksen, J. A., Gustin, M. S., Xin, M., Weisberg, P. J., and Fernandez, G. C. J. Air–soil exchange of
532 mercury from background soils in the United States, Sci. Total Environ., 366, 851–863, 2006.

533 Fa ï, X., Grangeon, S., Bahlmann, E., Fritsche, J., Obrist, D., Dommergue, A., Ferrari, C. P., Cairns, W.,
534 Ebinghaus, R., and Barbante, C. Diurnal production of gaseous mercury in the alpine snowpack
535 before snowmelt, J. Geophys. Res. Atmos., 112, 5671–5674, 2007.

536 Ferrari, C. P., Gauchard, P., Aspmo, K., Dommergue, A., Magand, O., Bahlmann, E., Nagorski, S.,
537 Temme, C., Ebinghaus, R., Steffen, A., Banic, C., Berg, T., Planchon, F., Barbante, C., Cescon, P.,
538 and Boutron, C. F. Snow–to–air exchanges of mercury in an Arctic seasonal snow pack in Ny-
539 Ålesund, Svalbard, Atmos. Environ., 39, 7633–7645, 2005.

540 Fitzgerald, W. F., and Gill, G. A. Subnanogram determination of mercury by two-stage gold
541 amalgamation and gas phase detection applied to atmospheric analysis, Anal. Chem., 51, 1714–
542 1720, 1979.

543 Fu, X. W., Feng, X., Liang, P., Deliger, Zhang, H., Ji, J., and Liu P. Temporal trend and sources of
544 speciated atmospheric mercury at Waliguan GAW station, northwestern China, Atmos. Chem.
545 Phys., 12, 1951–1964, 2012.

546 Fu, X. W., Feng, X. B., and Wang, S. F. Exchange fluxes of Hg between surfaces and atmosphere in the
547 eastern flank of Mount Gongga, Sichuan province, southwestern China, J. Geophys. Res. Atmos.,
548 113, D20, doi: 10.1029/2008JD009814, 2008a.

549 Fu, X. W., Feng, X. B., Zhu, W. Z., Wang, S. F., and Lu, J. Total gaseous mercury concentrations in
550 ambient air in the eastern slope of Mt. Gongga, South-Eastern fringe of the Tibetan plateau, China,
551 Atmos. Environ., 42, 970–979, 2008b.

552 Gabriel, M. C., and Williamson, D. G. Some insight into the influence of urban ground surface
553 properties on the air–surface exchange of total gaseous mercury, Appl. Geochem., 23, 794–806,
554 2008.

555 Gabriel, M. C., Williamson, D. G., and Brooks, S. Potential impact of rainfall on the air–surface
556 exchange of total gaseous mercury from two common urban ground surfaces, Atmos. Environ., 45,
557 1766–1774, 2011.

558 Gabriel, M. C., Williamson, D. G., Zhang, H., Brooks, S., and Lindberg, S. Diurnal and seasonal trends
559 in total gaseous mercury flux from three urban ground surfaces, Atmos. Environ., 40, 4269–4284,
560 2006.

561 Gillis, A., and Miller, D. R. Some potential errors in the measurement of mercury gas exchange at the
562 soil surface using a dynamic flux chamber, Sci. Total Environ., 260, 181–189, 2000.

563 Gustin, M. S., Biester, H., and Kim, C. S. Investigation of the light-enhanced emission of mercury from
564 naturally enriched substrates, Atmos. Environ., 36, 3241–3254, 2002.

565 Gustin, M. S., Engle, M., Ericksen, J., Lyman, S., Stamenkovic, J., and Xin, M. Mercury exchange
566 between the atmosphere and low mercury containing substrates, Appl. Geochem., 21, 1913–1923,
567 2006.

568 Gustin, M. S., Ericksen, J. A., Schorran, D. E., Johnson, D. W., Lindberg, S. E., and Coleman, J. S.
569 Application of controlled mesocosms for understanding mercury air–soil–plant exchange, Environ.
570 Sci. Technol., 38, 6044–6050, 2004.

571 Gustin, M. S., Lindberg, S., Marsik, F., Casimir, A., Ebinghaus, R., Edwards, G., Hubble-Fitzgerald, C.,
572 Kemp, R., Kock, H., Leonard, T., London J., Majewski, M., Montecinos, C., Owens, J., Pilote, M.,
573 Poissant, L., Rasmussen, P., Schaedlich, F., Schneeberger, D., Schroeder, W., Sommar, J., Turner,
574 R., Vette, A., Wallschlaeger, D., Xiao, Z., and Zhang, H. Nevada STORMS project: Measurement
575 of mercury emissions from naturally enriched surfaces, J. Geophys. Res. Atmos., 104, D17,
576 21831–21844, 1999.

577 Gustin, M. S., and Stamenkovic, J. Effect of watering and soil moisture on mercury emissions from
578 soils, Biogeochemistry, 76, 215–232, 2005.

579 Gustin, M. S., Taylor Jr, G. E., and Maxey, R. A. Effect of temperature and air movement on the flux of
580 elemental mercury from substrate to the atmosphere, J. Geophys. Res. Atmos., 102, 3891–3898,
581 1997.

582 Hintelmann, H., Harris, R., Heyes, A., Hurley, J. P., Kelly, C. A., Krabbenhoft, D. P., Lindberg, S.,
583 Rudd, J. W. M., Scott, K. J., and Louis, V. L. S. Reactivity and mobility of new and old mercury
584 deposition in a boreal forest ecosystem during the first year of the METAALICUS study, Environ.
585 Sci. Technol., 36, 5034–5040, 2002.

586 Huang, J., Kang, S. C., Wang, S. X., Wang, L., Zhang, Q. G., Guo, J. M., Wang, K., Zhang, G. S., and
587 Tripathee, L. Wet deposition of mercury at Lhasa, the capital city of Tibet, Sci. Total Environ., 447,
588 123–132, 2013.

589 Huang, J., Kang, S. C., Zhang, Q. G., Jenkins, M. G., Guo, J. M., Zhang, G. S., and Wang, K. Spatial
590 distribution and magnification processes of mercury in snow from high-elevation glaciers in the
591 Tibetan Plateau, Atmos. Environ., 46, 140–146, 2012.

592 Jiskra, M., Wiederhold, J. G., Skyllberg, U., Kronberg, R. M., Hajdas, I., and Kretzschmar, R. Mercury
593 deposition and re-emission pathways in boreal forest soils investigated with Hg isotope signatures,
594 Environ. Sci. Technol., 49, 7188–7196, 2015.

595 Johnson, D. W., Benesch, J. A., Gustin, M. S., Schorran, D. S., Lindberg, S. E., and Coleman, J. S.
596 Experimental evidence against diffusion control of Hg evasion from soils, Sci. Total Environ., 304,
597 175–184, 2003.

598 Kang, S. C., Xu, Y. W., You, Q. L., Flügel, W., Pepin, N., and Yao, T. D. Review of climate and
599 cryospheric change in the Tibetan Plateau, Environ. Res. Lett., 5, 015101, 2010.

600 Khwaja, A. R., Bloom, P. R., and Brezonik, P. L. Binding constants of divalent mercury (Hg^{2+}) in soil
601 humic acids and soil organic matter, Environ. Sci. Technol., 40, 844–849, 2006.

602 Kim, K. H., and Lindberg, S. E. Design and initial tests of a dynamic enclosure chamber for
603 measurements of vapor-phase mercury fluxes over soils, Water Air Soil Pollut., 80, 1059–1068,
604 1995.

605 Klusman, R. W., and Webster, J. D. Meteorological noise in crustal gas emission and relevance to
606 geochemical exploration, J. Geochem. Explor., 15, 63–76, 1981.

607 Kocman, D., and Horvat, M. A laboratory based experimental study of mercury emission from
608 contaminated soils in the River Idrijca catchment, Atmos. Chem. Phys., 10, 1417–1426, 2010.

609 Krabbenhoft, D. P., and Sunderland, E. M. Global change and mercury, Science, 341, 1457–1458, 2013.

610 Lalonde, J. D., Amyot, M., Doyon, M., and Auclair, J. Photo-induced Hg(II) reduction in snow from the
611 remote and temperate Experimental Lakes Area (Ontario, Canada), J. Geophys. Res. Atmos., 108,
612 471–475, 2003.

613 Lalonde, J. D., Poulain, A. J., and Marc, A. The role of mercury redox reactions in snow on snow–to–
614 air mercury transfer, Environ. Sci. Technol., 36, 174–178, 2001.

615 Lin, C. J., Gustin, M. S., Singhasuk, P., Eckley, C., and Miller, M. Empirical models for estimating
616 mercury flux from soils, Environ. Sci. Technol., 44, 8522–8528, 2010.

617 Lin, C. J., Zhu, W., Li, X. C., Feng, X. B., Sommar, J., and Shang, L. H. Novel dynamic flux chamber
618 for measuring air–surface exchange of Hg^0 from soils, Environ. Sci. Technol., 46, 8910–8920,
619 2012.

620 Lindberg, S. E., Zhang, H., Gustin, M., Vette, A., Marsik, F., Owens, J., Casimir, A., Ebinghaus, R.,
621 Edwards, G., Fitzgerald, C., Kemp, J., Kock, H. H., London, J., Majewski, M., Poissant, L., Pilote,
622 M., Rasmussen, P., Schaedlich, F., Schneeberger, D., Sommar, J., Turner, R., Wallschläger, D.,
623 and Xiao, Z. Increases in mercury emissions from desert soils in response to rainfall and irrigation,
624 J. Geophys. Res. Atmos., 104, 21879–21888, 1999.

625 Lindberg, S. E., Zhang, H., Vette, A. F., Gustin, M. S., Barnett, M. O., and Kuiken, T. Dynamic flux
626 chamber measurement of gaseous mercury emission fluxes over soils. Part 2: effect of flushing
627 flow rate and verification of a two-resistance exchange interface simulation model, Atmos.
628 Environ., 36, 847–859, 2002.

629 Loewen, M., Kang, S. C., Armstrong, D., Zhang, Q. G., Tomy, G., and Wang, F. Y. Atmospheric
630 transport of mercury to the Tibetan Plateau, Environ. Sci. Technol., 41, 7632–7638, 2007.

631 Malcolm, E. G., and Keeler, G. J. Measurements of mercury in dew: atmospheric removal of mercury
632 species to a wetted surface, Environ. Sci. Technol., 36, 2815–2821, 2002.

633 Mann, E. A., Mallory, M. L., Ziegler, S. E., Tordon, R., and O'Driscoll, N. J. Mercury in Arctic snow:
634 quantifying the kinetics of photochemical oxidation and reduction, Sci. Total Environ., 509–510,
635 115–132, 2015.

636 Mann, E., Ziegler, S., Mallory, M., and O'Driscoll, N. Mercury photochemistry in snow and
637 implications for Arctic ecosystems, Environ. Rev., 22, 331–345, 2014.

638 Mauclair, C., Layshock, J., and Carpi, A. Quantifying the effect of humic matter on the emission of
639 mercury from artificial soil surfaces. Appl. Geochem., 23, 594–601, 2008.

640 Mazur, M. E. E., Eckley, C. S., and Mitchell, C. P. J. Susceptibility of soil bound mercury to gaseous
641 emission as a function of source depth: an enriched isotope tracer investigation, Environ. Sci.
642 Technol., 49, 9143–9149, 2015.

643 Moore, C., and Carpi, A. Mechanisms of the emission of mercury from soil: Role of UV radiation, J.
644 Geophys. Res., 110, D24302, doi: 10.1029/2004JD005567, 2005.

645 NSIDC. National Snow and Ice Data Center, USA. www.nsidc.org.

646 Park, S. Y., Holsen, T. M., Kim, P. R., and Han, Y. J. Laboratory investigation of factors affecting
647 mercury emissions from soils, Environ. Earth Sci., 72, 2711–2721, 2014.

648 Peng, F., Xue, X., You, Q., Zhou, X., and Wang, T. Warming effects on carbon release in a permafrost
649 area of Qinghai-Tibet Plateau, Environ. Earth Sci., 73, 57–66, 2015a.

650 Peng, F., Xu, M., You, Q., Zhou, X., Wang, T., and Xue, X. Different responses of soil respiration and
651 its components to experimental warming with contrasting soil water content, Arct. Antarct. Alp.
652 Res., 47, 359–368, 2015b.

653 Pirrone, N., and Mason, R. P. (Eds). Hg fate and transport in the global atmosphere: emissions,
654 measurements and models, Springer: Geneva, 2009.

655 Poissant, L., Pilote, M., and Casimir, A. Mercury flux measurements in a naturally enriched area:
656 Correlation with environmental conditions during the Nevada Study and Tests of the Release of
657 Mercury From Soils (STORMS), J. Geophys. Res., 104, D17, 21845–21857, 1999.

658 Schuster, E. The behavior of mercury in the soil with special emphasis on complexation and adsorption
659 processes–a review of the literature, Water Air Soil Pollut., 56, 667–680, 1991.

660 Schlüter, K. Review: evaporation of mercury from soils. An integration and synthesis of current
661 knowledge, Environ. Geol., 39, 249–271, 2000.

662 Selin, N. E. Global biogeochemical cycling of mercury: A review, Annu. Rev. Env. Resour., 34, 43–63,
663 2009.

664 Sommar, J., Zhu, W., Lin, C. J., and Feng, X. Field approaches to measure mercury exchange between
665 natural surfaces and the atmosphere–a review, Crit. Rev. Environ. Sci. Technol., 43, 1657–1739,
666 2013.

667 Song, X., and Van Heyst, B. Volatilization of mercury from soils in response to simulated precipitation,
668 Atmos. Environ., 39, 7494–7505, 2005.

669 Sprovieri, F., Pirrone, N., Ebinghaus, R., Kock, H., and Dommergue, A. A review of worldwide
670 atmospheric mercury measurements, Atmos. Chem. Phys., 10, 8245–8265, 2010.

671 Steen, A. O., Berg, T., Dastoor, A. P., Durnford, D. A., Hole, L. R. and Pfaffhuber, K. A. Dynamic
672 exchange of gaseous elemental mercury during polar night and day, Atmos. Environ., 43, 5604–
673 561, 2009.

674 Streets, D. G., Hao, J., Wu, Y., Jiang, J., Chan, M., Tian, H., and Feng, X. Anthropogenic mercury
675 emissions in China, Atmos. Environ., 39, 7789–7806, 2005.

676 Toyota, K., McConnell, J. C., Staebler, R. M., and Dastoor, A. P.: Air–snowpack exchange of bromine,
677 ozone and mercury in the springtime Arctic simulated by the 1-D model PHANTAS – Part 1: In-
678 snow bromine activation and its impact on ozone, Atmos. Chem. Phys., 14, 4101–4133, 2014a.

679 Toyota, K., Dastoor, A. P., and Ryzhkov, A.: Air–snowpack exchange of bromine, ozone and mercury
680 in the springtime Arctic simulated by the 1-D model PHANTAS – Part 2: Mercury and its
681 speciation, Atmos. Chem. Phys., 14, 4135–4167, 2014b.

682 Wallschläger, D., Turner, R. R., London, J., Ebinghaus, R., Kock, H. H., Sommar, J., and Xiao, Z. F.
683 Factors affecting the measurement of mercury emissions from soils with flux chambers, J.
684 Geophys. Res., 104, D17, 21859–21871, 1999.

685 Wang, D. Y., He, L., Shi, X. J., Wei, S. Q., and Feng, X. B. Release flux of mercury from different
686 environmental surfaces in Chongqing, China, Chemosphere, 64, 1845–1854, 2006.

687 Wang, S. F., Feng, X. B., Qiu, G. L., Shang, L. H., Li, P., and Wei, Z. Q. Mercury concentrations and
688 air/soil fluxes in Wuchuan mercury mining district, Guizhou province, China, Atmos. Environ., 41,
689 5984–5993, 2007.

690 Wang, X. P., Yao, T. D., Wang, P. L., and Tian, L. D. The recent deposition of persistent organic
691 pollutants and mercury to the Dasuopu glacier, Mt. Xixiabangma, central Himalayas, Sci. Total
692 Environ., 394, 134–143, 2008.

693 Wei, K., Chen, W., and Huang, R. H. Long-term changes of the ultraviolet radiation in China and its
694 relationship with total ozone and precipitation, Adv. Atmos. Sci., 23, 700–710, 2006.

695 Xin, M., and Gustin, M. S. Gaseous elemental mercury exchange with low mercury containing soils:
696 Investigation of controlling factors, Appl. Geochem., 22, 1451–1466, 2007.

697 Xin, M., Gustin, M., and Johnson, D. Laboratory investigation of the potential for re-emission of
698 atmospherically derived Hg from soils, Environ. Sci. Technol., 41, 4946–4951, 2007.

699 Yang, Y. K., Zhang, C., Shi, X. J., Lin, T., and Wang, D. Y. Effect of organic matter and pH on
700 mercury release from soils, J. Environ. Sci., 19, 1349–1354, 2007.

701 Yin, X. F., Zhang Q. G., Tong Y. D., Zhang W., Wang X. J., Schauer J., and Kang S. C. Observations
702 of atmospheric mercury at a high altitude site in the Tibetan plateau in the winter of 2014/2015:
703 concentrations, speciation and insight into atmospheric hg in free troposphere, 12th International
704 Conference on Mercury as a Global Pollutant, 14–19 June, Jeju, Korea, 2015.

705 Zhang, H., and Lindberg, S. E. Processes influencing the emission of mercury from soils: A conceptual
706 model, J. Geophys. Res. Atmos., 104, 21889–21896, 1999.

707 Zhang, Q. G., Huang, J., Wang, F. Y., Mark, L., Xu, J. Z., Armstrong, D., Li, C. L., Zhang, Y. L., and
708 Kang, S. C. Mercury distribution and deposition in glacier snow over western China, Environ. Sci.
709 Technol., 46, 5404–5413, 2012.

710 Zhou, L., Zou, H., Shupo, M. A., and Peng, L. I. The Tibetan ozone low and its long-term variation
711 during 1979–2010, Acta Meteorol. Sin., 27, 75–86, 2013.

712 Zhu, J. S., Wang, D. Y., Liu, X., and Zhang, Y. T. Mercury fluxes from air/surface interfaces in paddy
713 field and dry land, Appl. Geochem., 26, 249–255, 2011.

714 Zhu, W., Lin, C.-J., Wang, X., Sommar, J., Fu, X., and Feng, X. Global observations and modeling of
715 atmosphere–surface exchange of elemental mercury: a critical review, Atmos. Chem. Phys., 16,
716 4451–4480, 2016.

717 Zhu, W., Sommar, J., Lin, C.-J., and Feng, X.: Mercury vapor air–surface exchange measured by
718 collocated micrometeorological and enclosure methods – Part I: Data comparability and method
719 characteristics, Atmos. Chem. Phys., 15, 685–702, 2015a.

720 Zhu, W., Sommar, J., Lin, C.-J., and Feng, X.: Mercury vapor air–surface exchange measured by
721 collocated micrometeorological and enclosure methods – Part II: Bias and uncertainty analysis,
722 Atmos. Chem. Phys., 15, 5359–5376, 2015b.

723

Atmos. Chem. Phys. Discuss., doi:10.5194/acp-2016-515, 2016
Manuscript under review for journal Atmos. Chem. Phys.
Published: 19 July 2016

Atmospheric Chemistry and Physics Discussions

724

725

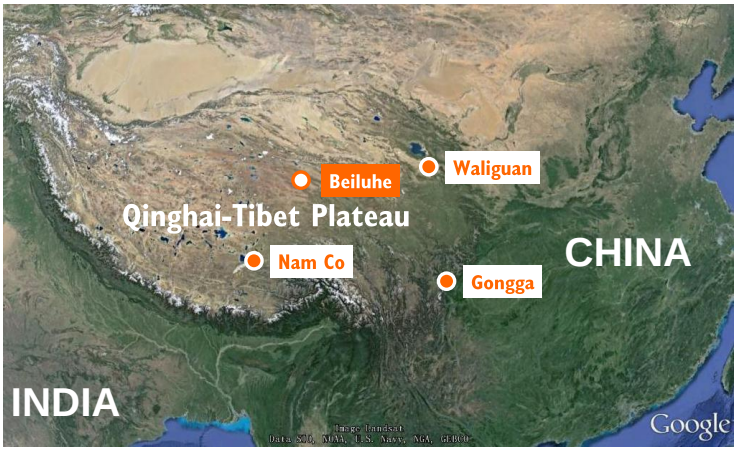

726

727

728 Figure 1. Locations of the Beiluhe station (4760 m a.s.l., this study), Mt. Waliguan (3816 m a.s.l., Fu et al., 2012), Mt.
729 Gongga (1640 m a.s.l., Fu et al., 2008b) and Nam Co (4730 m a.s.l., Yin et al., 2015) where atmospheric Hg were
730 determined.

Atmos. Chem. Phys. Discuss., doi:10.5194/acp-2016-515, 2016
Manuscript under review for journal Atmos. Chem. Phys.
Published: 19 July 2016

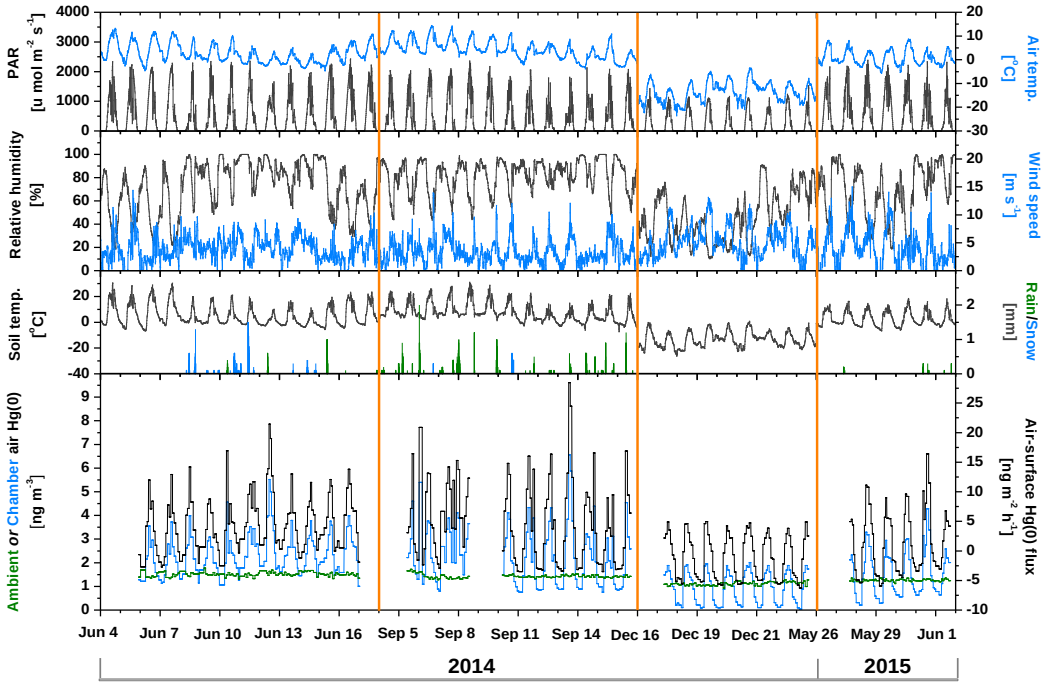

Figure 2. Temporal variation of environmental variables, air Hg(0) concentrations inside and outside of chamber, and air–surface Hg(0) flux at the Beiluhe station in the central QTP during four campaigns in 2014–2015.

Atmos. Chem. Phys. Discuss., doi:10.5194/acp-2016-515, 2016
Manuscript under review for journal Atmos. Chem. Phys.
Published: 19 July 2016

Atmospheric Chemistry and Physics Discussions

738

739

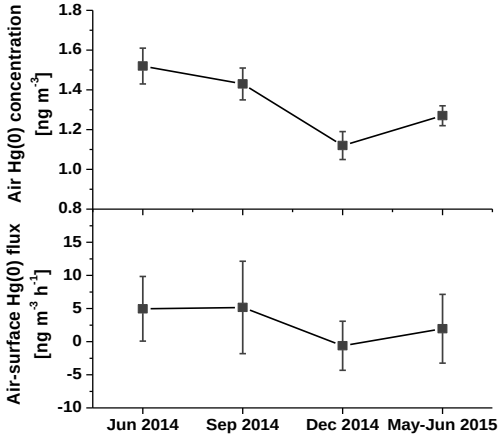

740

741

742 Figure 3. Seasonal variation of Hg(0) concentration in ambient air and air–surface Hg(0) flux during four campaigns at the
743 Beiluhe station in the central QTP in 2014–2015.

744

Atmos. Chem. Phys. Discuss., doi:10.5194/acp-2016-515, 2016
Manuscript under review for journal Atmos. Chem. Phys.
Published: 19 July 2016

Atmospheric Chemistry and Physics Discussions

745

746

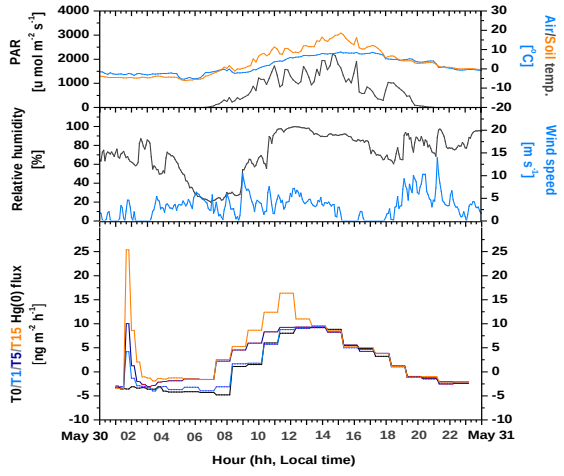

747

748

749 Figure 4. Temporal variation of Hg(0) flux over four soil plots with different treatment of water addition (T0: 0 mm
750 treatment, T1: 1 mm treatment, T5: 5 mm treatment and T15: 15 mm treatment) and the environmental variables.

751

Atmos. Chem. Phys. Discuss., doi:10.5194/acp-2016-515, 2016
Manuscript under review for journal Atmos. Chem. Phys.
Published: 19 July 2016

Atmospheric Chemistry and Physics Discussions

752

753

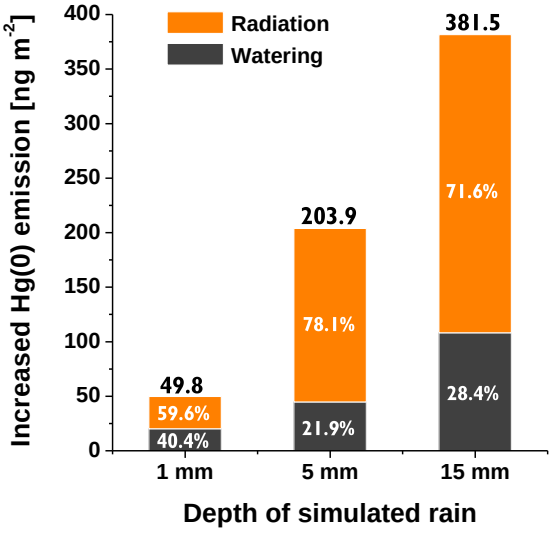

754

755

756 Figure 5. Increased Hg(0) emission for three different treatments (1 mm, 5 mm and 15 mm addition of water) compared with
757 the 0 mm treatment during the controlled experiment on 30 May 2015.

758

Atmos. Chem. Phys. Discuss., doi:10.5194/acp-2016-515, 2016
Manuscript under review for journal Atmos. Chem. Phys.
Published: 19 July 2016

Atmospheric Chemistry and Physics Discussions

759

760

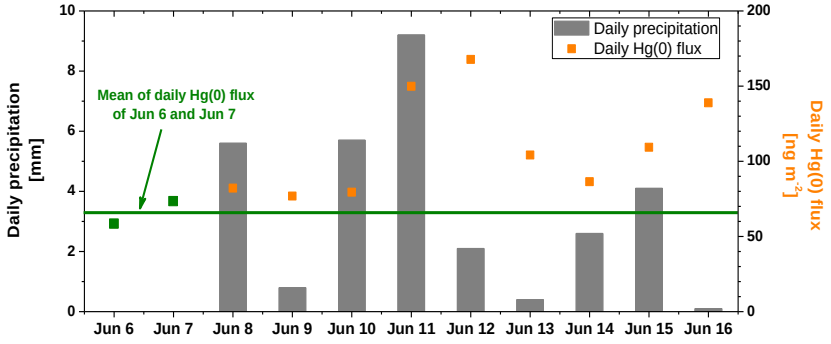

761

762

763 Figure 6. Daily Hg(0) flux and daily precipitation in June 2014 campaign.

764

Atmos. Chem. Phys. Discuss., doi:10.5194/acp-2016-515, 2016
Manuscript under review for journal Atmos. Chem. Phys.
Published: 19 July 2016

765

766

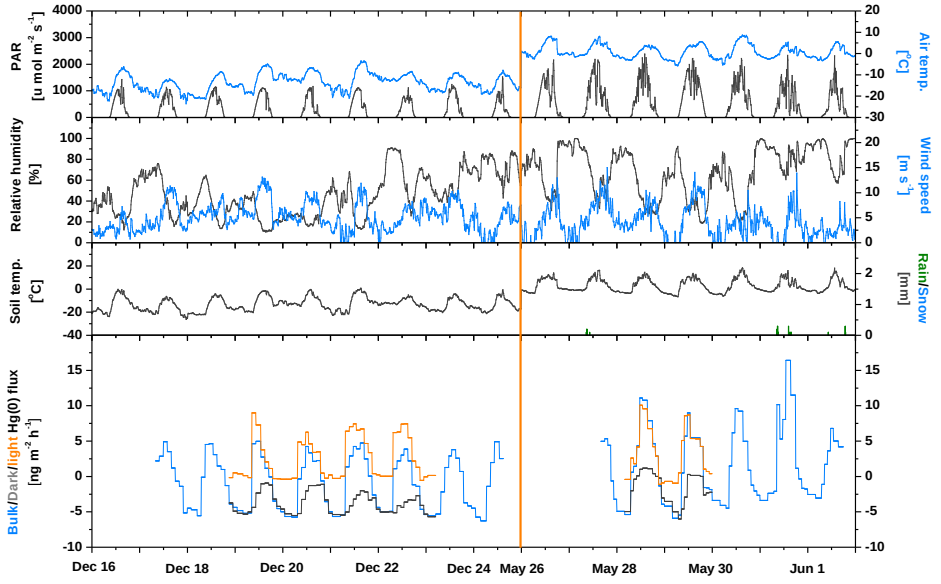

767

768

769 Figure 7. Temporal variation of bulk Hg(0) flux in the light, Hg(0) flux in the dark, and net Hg(0) flux in the light (bulk
770 Hg(0) flux in the light–Hg(0) flux in the dark) in six study days without precipitation during December 2014 campaign and
771 May–June 2015 campaign.

772

Atmos. Chem. Phys. Discuss., doi:10.5194/acp-2016-515, 2016
Manuscript under review for journal Atmos. Chem. Phys.
Published: 19 July 2016

Atmospheric Chemistry and Physics Discussions

773

774

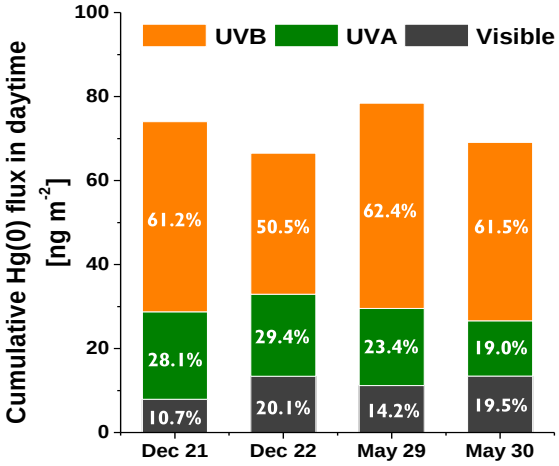

775

776

777 Figure 8. Cumulative Hg(0) emission flux in daytime triggered by UVB, UVA and visible light in four study days during
778 December 2014 campaign and May–June 2015 campaign. Four chambers with different exposure treatments were used to
779 measure Hg(0) flux simultaneously in the daytime. Chamber-A was used to measure the Hg(0) flux in the natural light.
780 Chamber-B and Chamber-C were covered with UVB filter and UV filters to remove the corresponding wavebands from the
781 natural light, respectively. Chamber-D covered with foil was used to measure Hg(0) flux in the dark. The experiments were
782 performed in four days without precipitation (21–22 December 2014 and 29–30 May 2015) to exclude the effect of
783 precipitation. Hg(0) flux triggered by UVB, UVA and visible light was equal to difference of flux between Chamber-A and
784 Chamber-B, between Chamber-B and Chamber-C, and between Chamber-C and Chamber-D, respectively. The transmittance
785 of UVB filter and UV filter was shown in Fig. S1 in Supplement.